화염배출 출구면적 변화에 대한 수직발사관 내부 초음속 충돌유동의 수치적 해석

이 광 섭[1], 홍 승 규[1], 안 창 수[1]

NUMERICAL INVESTIGATIONS OF SUPERSONIC JET IMPINGEMENT ON A FLAT WALL IN A CONFINED PLENUM

K. S. Lee, S. K. Hong and C. S. Ahan

Viscous solutions of supersonic jet impinging on a flat wall in a confined plenum are simulated using three-dimensional Navier-Stokes solver. A confined plenum was designed for simulating the missile launch and analyzing the behavior of the exhaust plume, which were accompanied by complex flow interactions with shock and boundary layer.

Concerns of this paper are to show accurate simulation of internal flow in confined plenum and to demonstrate the jet flow structure when the jet interacts with a small opening on the side. Objectives of this numerical simulation are to understand the effect of changing the plume exit area of the plenum. Pressure and temperature rise at certain position in the plenum are traced and compared with test data.

Key Words: Nozzle flow, Supersonic Jet Impingement, Shock wave, Plume Exhaust Area

1. Introduction

Numerical study of VLS flow is carried out using a three-dimensional Navier-Stokes solver incorporating the Characteristic Flux Difference Splitting (CFDS) method. CFDS method, a variant of Roe's flux-difference splitting formulation, has been developed formerly as a viable engineering prediction tool for aerodynamic design and had indeed shown its versatility in computing complex flows. The CFDS method, however, being rooted from Roe's flux-difference is also susceptible to the carbuncle problem. In the VLS flow computation, as the jet exit pressure becomes greater, 'carbuncle phenomenon' has been encountered during numerical calculation. This shock instability problem has been cured and the current code is then applied to solve the flow in a scaled-down VLS geometry instead of a full-scale VLS configuration. The complex flow inside the VLS is visualized and the solutions are utilized in determining the plume exhaust area of the plenum.

2. Numerical Method

The Characteristic Flux Difference Splitting (CFDS), numerical method for the three-dimensional Navier-Stokes has been applied to various complex flows and validated over the past few years [1-3]. In the present study for supersonic jet impingement calculations, the entropy fixing formula is used to prevent shock instability.

3. Results and Discussions

A module of VLS contains eight missiles in a plenum vertically. But for cost-saving purpose there is a need for testing

1 국방과학연구소

scaled-down version of VLS containing a single rocket motor instead of eight rocket motors. The main purposes of this test are fist to prove the material integrity on the plenum wall during the missile launching process and second to see the discharge of plume gas through the plume exhaust area. In the present study, the focus is to understand the flow structure and to see the pressure increase in the plenum for varied plume exhaust area.

The computational grid system for flow simulation of VLS consists of 720,000 grid points as shown Fig. 1 with 9 blocks. Every block is overlapped with neighboring blocks. Coordinate system is denoted in Fig.1 pointing y-axis upward and x-direction horizontal which is plume exhaust direction. A schematic view of the plenum exhaust area is shown in Fig.2. The 'Plume Exhaust Area' is shown as in Fig. 2 with area ratio 17.1. The area ratio is defined as the plume exhaust area divided by nozzle exit area. The area ratio varies from 1.8 to 17.1. Typical flow solutions are shown for the area ratio 17.1 case. In order to predict the average pressure in the plenum, pressure histories at several points in the plenum are traced and averaged. The plenum is surrounded by solid wall except plume exhaust area in x-direction. Figure 3 and Fig. 4 show grid of yz-plane view and xy-plane view, respectively, cutting through the motor. The yz-plane is a closed space and xy-plane contains plume exhaust area as sketched in Fig.4 with solid line. This VLS design challenge is to safely discharge the rocket exhaust gas during the rocket motor test. Thus, it is important to know the overall pressure level in the plenum chamber lest the exit area small enough to allow pressure build-up.

Mach contours of the yz-plane view and xy-plane view are plotted in Fig.5 and Fig.6 respectively. The yz-plane is a geometrically symmetric plane. Therefore the Mach contours show symmetric shape. Figure 5 shows well-developed Mach disk and wall jet on the bottom wall. In case of xy-plane as shown in Fig. 6, Mach disk is not solid, which means the flow oscillates toward left and right with periodic motion. These oscillations of shock shell are observed during the numerical calculation in x-direction. The maximum Mach in the main jet is about 4.0 and the wall jet Mach is 2.0. The speed of the front of exhaust plume through the exit area is about Mach 1.0 as shown in Fig. 6. The characteristics of flow structure in the xy-plane is highly unsteady compared with those of in the yz-plane. Two circulations in yz-plane are shown as in Fig. 5 with steady state while a circulation on the left side of the xy-plane remains but disappears with unsteady state. Figure 7 and Fig. 8 show pressure contours in yz-plane and xy-plane respectively. The pressure levels are denoted from 0 to 5.0 atmosphere in order to show contour lines clearly. The average pressure in the plenum is 1.7 atmosphere except the main jet impinging region. The maximum pressure under the nozzle exit is about 10 atm. on average according to the numerical iteration. Also the pressure at the main jet impinging zone fluctuates with certain frequency. The temperature contours in yz-plane and xy-plane are plotted in Fig.9 and Fig.10 respectively. The maximum temperature near the side wall reaches 1,100 K as shown in Fig.9. Velocity vectors with stream lines are plotted in Fig.11 and Fig. 12 exhibiting several recirculation regions near the main jet stream as shown in Fig. 11 and plume exhaust as shown in Fig. 12. Steady state flow structure in yz-plane is shown as in Fig.11with symmetric flow patterns. Stream lines in plume exhaust direction are shown as in Fig.12.

Fig.13 and Fig.14 show Mach contours and temperature contours in zy-plnae view cutting through plenum horizontally in the middle of the plenum chamber. The shock shell formation is shaped non-circular even though the rocket motor nozzle shape is circular. This noncircular shock shell is due to the surrounded side wall effect. Generally in jet impinging on flat plate, the shape of the shock shell is circular. Mach contours in Fig. 13 and temperature contours in Fig. 14 both show noncircular shock shell. The average pressure in the plenum for varied area ratio is plotted in fig.15. Steady pressure rise in plenum is observed during numerical iteration below area ratio 10.0 because of insufficient exhaust space.

Figure 16 reveals the magnitude of ablation on the bottom wall after the motor test. This ablation shape is very similar to the Mach and temperature distributions as shown in Fig.13 and Fig. 14. Figure 17 displays the facilities of the test motor and test set up. Temperature sensors are located on the plenum chamber as shown in Fig.18(a) with three gages and the measured temperatures are plotted in Fig 8(b) with solid line and calculated maximum temperature with symbolic notation. Calculated temperatures are reasonably matched with measured data except T3. The reason of this mismatch is not yet clear.

4. Conclusions

Navier-Stokes calculations are performed using scaled-down VLS plenum for specific design purpose. Flow structures with area ratio 17.1 are presented for several planes. The average pressure under the jet center is 10.0 atm. The average pressure in the plenum chamber is below 2.0 atm. and plume gas goes well through the exhaust space in a area ratio 17.1 case but steady increase in pressure is observed with the area ration 10 or less. Two symmetric recirculation zones in yz-plane are observed and the shock shell oscillation in xy-direction is also observed. The frequency of the shock shell fluctuation is about 10 kHz.

5. References

[1] Hong, S. K., and Lee, K. S., 1997, "Simulation of Jet Plume Impinging onto a Duct," ISABE 97-7184, *AIAA ISOABE* (International Society for Air Breathing Engines) Symposium Papers, Sept. 7-12, 1997, p.1359-1365.

[2] Kwang-Seop Lee, Seung-Kyu Hong and Seung-O Park, 2004, "Supersonic Jet Impingement Navier-Stokes Computations for Vertical Launching System Design Applications," *Journal of Spacecraft and Rockets,* Vol.41, No.5, 2004, p.735-744.

[3] Lee, K.S., Hong, S.K., and Park, S.O, 2001, "Improvement in Flux-Difference Splitting Algorithm for Accurate and Robust Flow Simulation," *Computational Fluid Dynamics Journal, Japan,* Vol.10, No.2, *Proc. 41SCFD-Davis,* Vol.2, (1991), p.13-23.

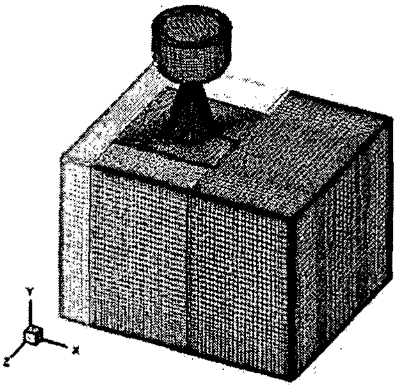

Fig. 1. Computational grid topology for VLS analysis.

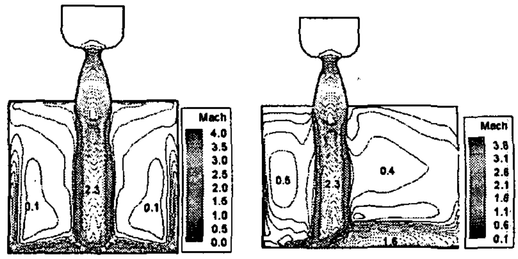

Fig. 5. Mach contours in yz-plane(left)
Fig. 6. Mach contours in xy-plane(right)

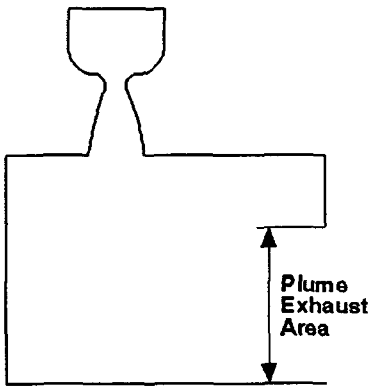

Fig. 2. Schematic view of exhaust area.

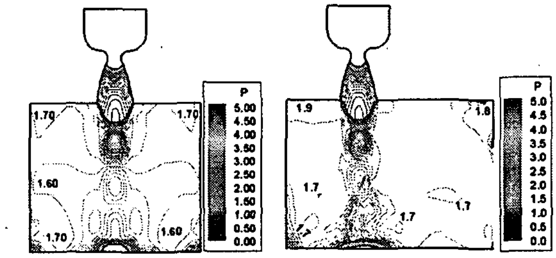

Fig. 7. Pressure contours in yz-plane(left)
Fig. 8. Pressure contours in xy-plane(right)

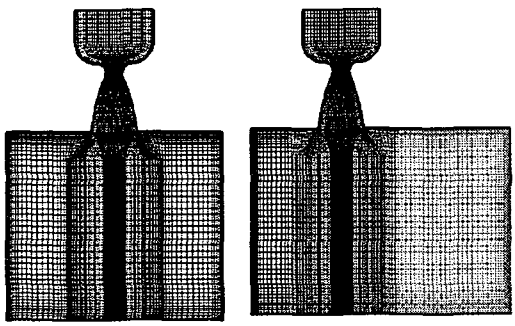

Fig. 3. yz-plane view of grid system(left)
Fig. 4. xy-plane view of grid system(right)

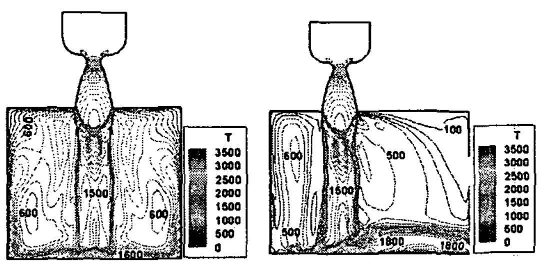

Fig. 9. Temperature contours in yz-plane(left)
Fig. 10. Temperature contours in xy-plane(right)

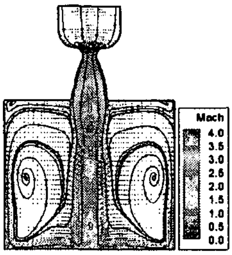

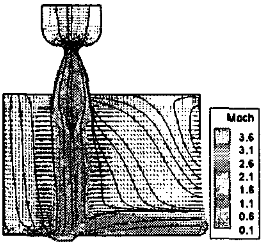

Fig. 11. *Stream lines in yz-plane(left)*
Fig. 12. Stream lines in xy-plane(right)

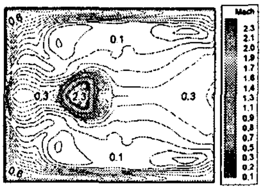

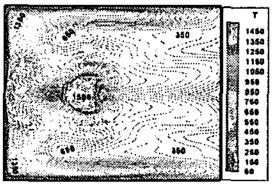

Fig. 13. Mach contours in xz-plane.(left)
Fig. 14. Temperature contours in xz-plane.(right)

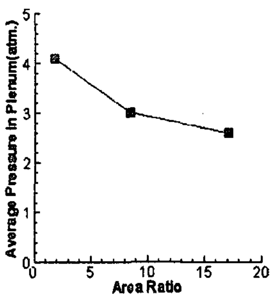

15. Average pressure in plenum for varied area ratio

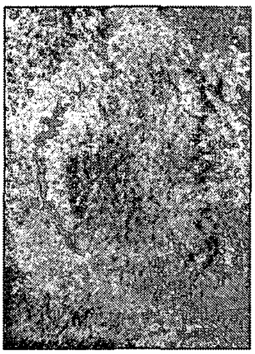

Fig. 16. Ablations after motor test.

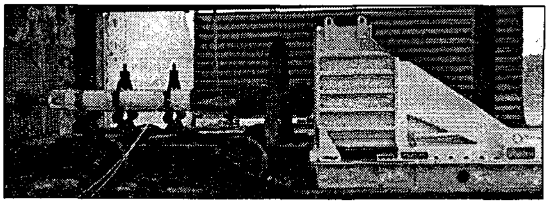

Fig. 17. Photograph of motor test facilities

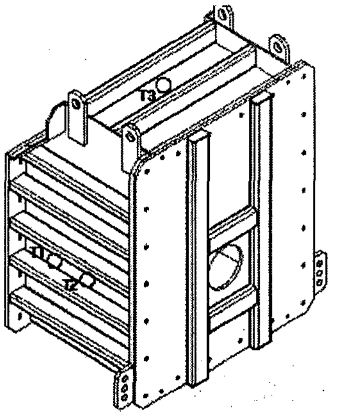

(a) Sensor locations for T1, T2, T3

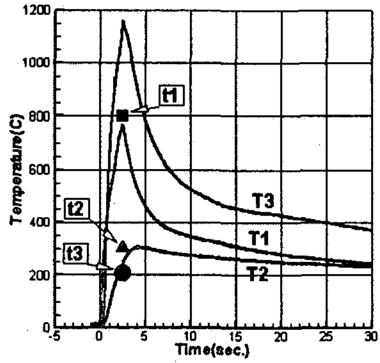

(b) Measured (T1,T2,T3) and computed (t1,t2,t3) values

Fig. 18 Temperature measurement positions with three gages(a) and compares of values(b).